MOEM

Modern Electronic Materials 2021; 7(3): 109–113
DOI 10.3897/j.moem.7.3.74274

Research Article

# Two-dimensional $WSe_2$ flakes under high power optical excitation

Kirill Brekhov[1], Sergey Lavrov[1], Andrey Kudryavtsev[1], Nikita Ilyin[1]

*1 MIREA – Russian Technological University, 78 Vernadsky Ave., Moscow 119454, Russia*

Corresponding author: Sergey Lavrov (sdlavrov@mail.ru)

**Received** 4 September 2021 ♦ **Accepted** 11 September 2021 ♦ **Published** 30 September 2021

**Citation:** Brekhov K, Lavrov S, Kudryavtsev A, Ilyin N (2021) Two-dimensional $WSe_2$ flakes under high power optical excitation. Modern Electronic Materials 7(3): 109–113. https://doi.org/10.3897/j.moem.7.3.74274

## Abstract

Quasi-2D layers of transition metal dichalcogenides are promising candidates for creating saturable absorbers for pulsed lasers. However, the peculiarities of intense electromagnetic radiation's influence on such structures have not been thoroughly studied. This paper explores the dynamics of photoexcited carriers in $WSe_2$ flakes through experimental studies. These studies found that $WSe_2$ flakes significantly change their optical properties under the influence of a high-power optical pump, allowed estimating the thermalization time of these structures (about 2 ps), and found that full relaxation takes more than 10 ps. The concentration of carriers in the semiconductor surface layer was estimated to be about $10^{28}$ $m^{-3}$. It was found that standard description models of the optical response based on exciton resonances and absorption by free carriers could not adequately describe the experiments' results. Thus, for an accurate description of the optical response, it was necessary to consider the effects associated with Coulomb screening that are caused by the high concentration of photo-excited carriers of the optical pumping densities used in this experiment.

## Keywords

carriers lifetime, graphene-like semiconductors, time-resolved spectroscopy, transition metal dichalcogenides.

## 1. Introduction

After their discovery, transition metal dichalcogenides **(TMD)** became highly promising 2D materials for nanoelectronics devices. The explosive interest in such structures is primarily due to their unique properties, including the presence of a direct nonzero bandgap, real two-dimensionality, chemical and thermal stability, and flexibility. The possibility of these materials' application in various fields of nano- and optoelectronics, from logic devices [1, 2] and memory cells [3, 4] to biosensors [5] and gas sensors [6], has been demonstrated.

Another promising application of these materials is the creation of saturable absorbers working both in the visible [7, 8] and infrared optical ranges [9]. The possibility of applying these materials as filters is related to their very high nonlinear optical absorption [10]. Therefore, such saturable absorbers can be used both in mode-locking and in Q-switching [11–13] methods. However, the physical mechanisms of such saturated absorbers under the influence of high-intensity optical fields have not been thoroughly investigated.

Quasi-2D structures based on transition metal dichalcogenides are promising objects for studying the optical response to high-intensive pulsed laser radiation, both from fundamental and applied perspectives. At high pump powers, the effects caused by an increase in the photoexcited carriers' concentration, such as the occurrence of an electron-hole plasma regime and the disappearance

of exciton resonances, become critical. Thus, investigating changes in the optical response occurring under these conditions is essential for photonics' development.

We present our results of photo-induced optical properties' changes in $WSe_2$ flakes under ultra-short and high-power optical pulses.

## 2. Materials and methods

Experimental studies of photoexcited carriers' relaxation in $WSe_2$ flakes were performed by time-resolved spectroscopy. This technique makes it possible to study processes occurring in various materials under the action of ultra-short laser pulses in the sub-picosecond time frame.

A modified pump-probe technique was used for the experimental studies [14, 15]. Radiation with a wavelength of 400 nm (photon energy 3.1 eV) was used as a pump, which allowed effective carriers excitation from the valence band into the conduction band. Radiation with a wavelength of 800 nm (photon energy 1.55 eV) was used as a probe. This wavelength was chosen due to the bandgap's width of the specified material, which is about 1.97 eV. The radiation energy density on the sample was as follows: excitation – 70 mJ/cm$^2$, and probing – 5 mJ/cm$^2$. Both beams were focused on the sample by the collinear scheme with an objective lens multiplicity ×40. The reflected probe beam was then focused on the photodiode.

Due to the use of a lens with a high numerical aperture and pumping radiation with high peak power in this study, the resulting energy density was much higher than those of similar studies [16, 17]. To prevent sample destruction under the influence of such powerful radiation, the pulse repetition rate was additionally diluted to 3 kHz.

Quasi-2D TMD flakes were made by the standard technique of mechanical exfoliation from bulk $WSe_2$ crystal. Such bulk structures are now widespread and therefore commercially available. A $Si/SiO_2$ plate with an oxide thickness of 90 nm was used as a substrate, which provided the highest optical contrast [18].

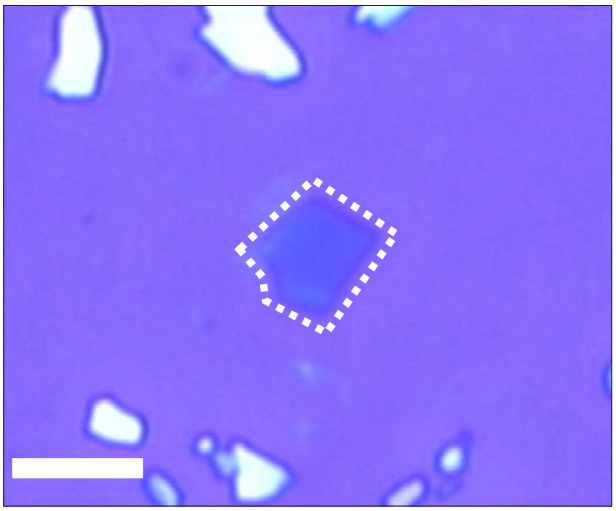

**Figure 1.** Optical image of the $WSe_2$ flake. The length of the scale bar is 5 μm. Dotted line shows 2D $WSe_2$ flake.

A $WSe_2$ flake with a thickness of about 20 nm (25 monolayers) was selected to avoid any substrate contributions to the investigated optical processes. This thickness ensures almost complete absorption of pump optical radiation in the layer and completely excludes any substrate contributions. Thus, for a given thickness of TMD, considering multi-beam interference, it was estimated that the silicon wafer would absorb less than 5% of the incident light. However, it was also found that TMD monolayered flakes, in addition to a small optical signal compared to the substrate contribution, quickly degenerate under the action of the powerful optical pump used in this work.

The optical image of the investigated quasi-2D sample is shown in Fig. 1. The flake size was about 5 × 5 μm, which was enough to focus the optical radiation only on the investigated flakes to avoid any silicon contributions.

All experimental works (the creation and study of 2D materials) were made by authors in the research laboratory of the Nanoelectronics Department, Institute of Physics and Technology, RTU MIREA.

## 3. Results and discussion

The dynamics of the excitation and subsequent relaxation of the quasi-2D $WSe_2$ electronic subsystem were investigated using the time-resolved spectroscopy method. The results of the experiment are shown in Fig. 2. The dependence of photo-induced reflectivity change for probe wavelength, depending on the time delay between pulses for different pump energy densities, is presented. The studies were conducted in the time range of up to 10 ps. The number of experimental points for convenience was reduced when visualizing the obtained data.

As shown, after a sharp initial excitation for a time of the order of the pulse duration (about 35 fs), the signal exponentially relaxed (Fig. 2).

We used the approach proposed in [19] to describe the relaxation of the photoexcited electron subsystem in semiconductor materials and to determine the relaxation time. The following expression approximated the experimental dependences shown in Fig. 2:

$$y = A\exp\left(-\frac{\tau_d^2}{4\omega^2}\right) + B\exp\left(\frac{\omega^2}{\tau_1^2}-\frac{\tau_d}{\tau_1}\right)\left[1-\mathrm{erf}\left(\frac{\omega}{\tau_1}-\frac{\tau_d}{2\omega}\right)\right] + C\exp\left(\frac{\omega^2}{\tau_2^2}-\frac{\tau_d}{\tau_2}\right)\left[1-\mathrm{erf}\left(\frac{\omega}{\tau_2}-\frac{\tau_d}{2\omega}\right)\right], \quad (1)$$

where $\tau_d$ is delay time between pulses, $\tau_1$, $\tau_1$ is relaxation times, $A$, $B$ and C is amplitudes, $\omega$ is pulse width.

The first term of this expression describes the excitation of the sample electronic subsystem by a femtosecond

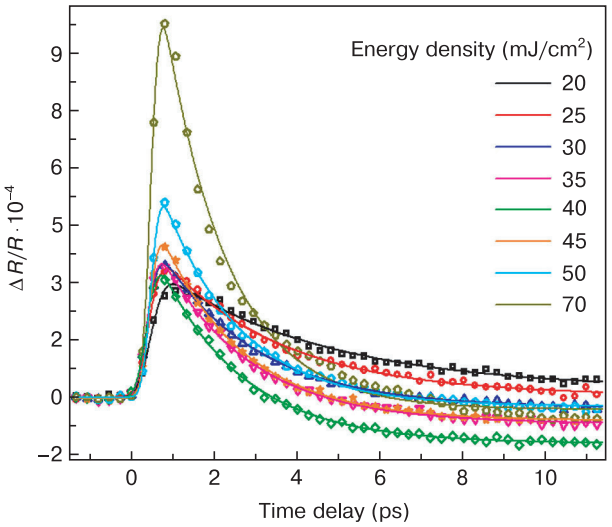


**Figure 2.** Photo-induced change of $WSe_2$ flake reflectivity for different pump powers. Solid lines – the result of approximation.

laser pulse, and the second and third terms describe the relaxation processes of the sample electronic subsystem with $\tau_1$ and $\tau_2$ times, respectively. According to the literature data, time $\tau_1$ corresponds to the thermalization process (the distribution of photoexcited carriers along sublevels in the conduction band) and time $\tau_2$ corresponds to the recombination time of photoexcited carriers from the conduction band to the valence band [20].

Using the approximation, it was found that the thermalization time of photo-excited carriers in the studied $WSe_2$ flake was about 2 ps. However, based on the presented experimental dependencies, the characteristic recombination time $\tau_2$ could not be determined because it significantly exceeded 10 ps.

In the case of low optical power carriers with energies much higher than the energy of exciton resonances were generated. Consequently, electrons and holes relaxed, moving in momentum space to the conduction band's minimum and the valence band's maximum, respectively, after which they formed excitons. Similar processes have been partially investigated and described in [21].

Notably, the energy of the probing radiation was 1.55 eV, which was approximately equal to the value of exciton resonance in the investigated sample. Further, the optical response decreased due to carrier recombination, and the characteristic lifetime of excitons exceeded the maximum experimental delay time.

In the presence of exciton states, the sample optical response can be described using the model proposed in [14]. Moreover, it allowed determining the regularities of optical coefficients change for semiconductor materials (and, respectively, the induced reflectivity).

This model roughly divides the general dielectric function of a semiconductor into two ranges: high-energy and low-energy. The high-energy range corresponds to inter-zone transitions in semiconductors, and the low-energy range corresponds to exciton transitions. There were two main exciton transitions for the considered bulk $WSe_2$ crystal at room temperature: *A* (1.65 eV) and *B* (2.08 eV) [22]. In the case under consideration, the A-exciton was the closest to the probing radiation energy, and it give the determining contribution to the induced reflection coefficient.

In general, the characteristic values of the differential reflection coefficient and peculiarities of its dynamics in this experiment were due to several effects of a dramatic increase in the concentration of photo-excited carriers. The concentration of photoexcited carriers in a thin near-surface layer can be estimated based on a simple ratio:

$$N_s = \alpha\left(1-R_I\right)\frac{f}{E}, \tag{2}$$

where the following parameters of pump radiation are used: α is absorption coefficient, $R_I$ is reflection coefficient, $f$ is power density, and $E$ is photon energy [23].

According to this formula, the carrier concentration in the near-surface layer for the pump power density used was about $10^{22}$ $cm^{-3}$. This value was quite large and exceeded the values of Mott concentration in bulk and monolayer samples of transition metal dichalcogenides known from other works [24, 25].

The Mott density is the characteristic carrier density at which the transition from the exciton regime to the electron-hole plasma regime occurs, where free carriers predominate. Thus, there is a change of exciton resonances' position, they further decrease, and then they completely disappear due to screening of Coulomb's attraction between oppositely charged carriers.

Therefore, instead of using the model described above, the optical response features in our experiment are described considering the effects associated with high free carrier densities: the bandgap renormalization effect and the band-filling effect.

The need to consider the mentioned effects was also confirmed by the fact that the estimation of the differential reflection coefficient considering only free-carrier absorption (according to the Drude model) did not converge with the experimental results.

According to the Drude model, the dielectric permittivity of the excited sample was

$$\varepsilon = \varepsilon_{\text{core}} + \frac{4\pi i}{\omega}\frac{Ne^2\tau}{m\left(1-i\omega\tau\right)}, \tag{3}$$

where $\varepsilon_{\text{core}}$ is dielectric permittivity of a non-excited sample, ω is probe radiation frequency, τ is carriers relaxation time, $N$ is concentration of photo-excited carriers, $m$ is effective mass.

In the band-filling effect, also known as the Burstein–Moss effect [26], the concentration of carriers increased, and the electrons from the valence band need energies that exceed the nominal bandgap (as well as the holes when they get from the conduction band into the valence band) to get into the conduction band. This effect leads to a decrease in the absorption coefficient at photon energies

exceeding the bandgap. As the concentration of carriers increases, the absorption coefficient becomes negative, i.e., instead of absorbing radiation, its amplification is observed.

The effect of bandgap renormalization occurred because the injected electrons that were concentrated in the lower part of the conduction band (as well as holes in the upper part of the valence band) were repelled from one another due to the Coulomb interaction. Additionally, electrons with the same spin projection avoid one another for statistical reasons, which leads to a decrease in the bottom of the conduction band (similarly, in the case of holes, it raises the ceiling of the valence band). The combination of these effects led to a bandgap reduction.

Thus, for a full description of the optical response dynamics under these conditions, further experiments are required to provide complete information about the effects associated with the presence of dense electron-hole plasma in the TMD.

# 4. Conclusions

This work, involved an experimental study of the effect of high-powered optical radiation of the order of several tens of mJ/cm$^2$ on quasi-2D $WSe_2$ films. A significant change in the optical response under pump radiation was revealed. Based on the results of reflectivity measurements, the estimation of characteristic relaxation and the recombination times of photo-excited carriers were made: thermalization time was about 2 ps; recombination time was >10 ps.

The estimation of the photoexcited carriers' concentration in the surface layer about $10^{28}$ m$^{-3}$. Through this connection, it was shown that at the given radiation power densities for an adequate description of optical response, it is necessary to consider the disappearance of exciton resonances due to Coulomb screening and other effects becoming essential at high carriers' concentrations, such as the band-filling effect and bandgap renormalization. Further experimental studies of these samples are planned to build a theoretical model explaining changes in optical parameters arising under these conditions.

# Acknowledgements

This work was supported by the Ministry of Education and Science of the Russian Federation (state task № FSFZ-0706-2020-0022). The works were partially performed using the equipment of the RTU-MIREA research resource center.

# References

1. Jang H., Liu C., Hinton H., Lee M.-H., Kim H., Seol M., Shin H.-J., Park S., Ham D. An atomically thin optoelectronic machine vision processor. Adv. Mater., 2020; 32(36): 2002431. http://dx.doi.org/10.1002/adma.202002431
2. Liu Y., Wang P., Wang Y., Huang Y., Duan X. Suppressed threshold voltage roll-off and ambipolar transport in multilayer transition metal dichalcogenide feed-back gate transistors. *Nano Res.*, 2020; 13(7): 1943–1947. http://dx.doi.org/10.1007/s12274-020-2760-6
3. Kim R.H., Lee J, Kim K.L., Cho S.M., Kim D.H., Park C. Flexible nonvolatile transistor memory with solution-processed transition metal dichalcogenides. *Small*, 2017; 13(20): 1603971. http://dx.doi.org/10.1002/smll.201603971
4. Abdullaev D.A., Milovanov R.A., Volkov R.L., Borgardt N.I., Lantsev A.N., Vorotilov K.A., Sigov A.S. Ferroelectric memory: state-of-the-art manufacturing and research. *Russ. Technol. J.*, 2020; 8(5): 44–67. (In Russ.). http://dx.doi.org/10.32362/2500-316X-2020-8-5-44-67
5. Hu Y., Huang Y., Tan C., Zhang X., Lu Q., Sindoro M., Huang X., Huang W., Wang L., Zhang H. Two-dimensional transition metal dichalcogenide nanomaterials for biosensing applications. *Mater Chem Front.*, 2017; 1(1): 24–36. http://dx.doi.org/10.1039/c6qm00195e
6. Järvinen T., Lorite G.S., Peräntie J., Toth G., Saarakkala S., Virtanen V.K., Kordas K. $WS_2$ and $MoS_2$ thin film gas sensors with high response to $NH_3$ in air at low temperature. *Nanotechnology*, 2019; 30(40): 405501. http://dx.doi.org/10.1088/1361-6528/ab2d48
7. Luo Z., Wu D., Xu B., Xu H., Cai Z., Peng J., Weng J., Xu S., Zhu C., Wang F., Sund Z., Zhange H. Two-dimensional material-based saturable absorbers: Towards compact visible-wavelength all-fiber pulsed lasers. *Nanoscale*, 2016; 8(2): 1066–1072. http://dx.doi.org/10.1039/c5nr06981e
8. Zou J., Ruan Q., Zhang X., Xu B., Cai Z., Luo Z. Visible-wavelength pulsed lasers with low-dimensional saturable absorbers. *Nanophotonics*, 2020; 9(8): 2273–2294. http://dx.doi.org/10.1515/nanoph-2020-0022
9. Guo C., Wei J., Yan P., Luo R., Ruan S., Wang J., Guo B., Hua P., Lue Q. Mode-locked fiber laser at 2.8 μm using a chemical-vapor-deposited $WSe_2$ saturable absorber mirror. *Appl. Phys. Express*, 2020; 13(1): 012013. http://dx.doi.org/10.7567/1882-0786/ab6031
10. Pang L., Liu W., Tian W., Han H., Wei Z. Nanosecond hybrid Q-switched Er-doped fiber laser with $WS_2$ saturable absorber. *IEEE Photonics J.*, 2016; 8(3): 1–7. http://dx.doi.org/10.1109/JPHOT.2016.2574333
11. Chen B., Zhang X., Wu K., Wang H., Wang J., Chen J. Q-switched fiber laser based on transition metal dichalcogenides $MoS_2$, $MoSe_2$, $WS_2$, and $WSe_2$. *Opt. Express*, 2015; 23(20): 26723. http://dx.doi.org/10.1364/oe.23.026723
12. Mohanraj J., Velmurugan V., Sivabalan S. Transition metal dichalcogenides based saturable absorbers for pulsed laser technology. *Opt. Mater.*, 2016; 60: 601–617. http://dx.doi.org/10.1016/j.optmat.2016.09.007
13. Li Z., Dong N., Zhang Y., Wang J., Yu H., Chen F. Invited article: Mode-locked waveguide lasers modulated by rhenium diselenide as

a new saturable absorber. *APL Photonics*, 2018; 3(8): 080802. http://dx.doi.org/10.1063/1.5032243

14. Shestakova A., Lavrov S., Brekhov K., Ilyin N., Kudryavtsev A., Mishina E.D., Kulyuk L.L. Photoexcitation carrier kinetics in $WSe_2$ nanolayers in the vicinity of the band edge. *Phys. Status Solidi*, 2018; 255(1): 1700259. http://dx.doi.org/10.1002/pssb.201700259
15. Khorrami Gh.H., Mousavi M., Khayatian S.A., Kompany A., Khorsand Zak A. Green synthesis and characterization of $ANbO_3$ (A = Na, K) nanopowders fabricated using a biopolymer. *Int. J Mod. Phys. B*, 2017; 31(27): 1750194. http://dx.doi.org/10.1142/S0217979217501946
16. Cui Q., Ceballos F., Kumar N., Zhao H. Transient absorption microscopy of monolayer and bulk $WSe_2$. *ACS Nano*, 2014; 8(3): 2970–2976. http://dx.doi.org/10.1021/nn500277y
17. Valencia-Acuna P., Zereshki P., Tavakoli M.M., Park J.H., Kong J., Zhao H. Transient absorption of transition metal dichalcogenide monolayers studied by a photodope-pump-probe technique. *Phys. Rev. B*, 2020; 102(3): 035414. http://dx.doi.org/10.1103/PhysRevB.102.035414
18. Li H., Wu J., Huang X., Lu G., Yang J., Lu X., Xiong Q., Zhang H. Rapid and reliable thickness identification of two-dimensional nanosheets using optical microscopy. ACS Nano, 2013; 7(11): 10344–10353. http://dx.doi.org/10.1021/nn4047474
19. Kimel A.V., Bentivegna F., Gridnev V.N., Pavlov V.V., Pisarev R.V., Rasing Th. Room-temperature ultrafast carrier and spin dynamics in GaAs probed by the photoinduced magneto-optical Kerr effect. *Phys. Rev. B*, 2001; 63(23): 2352011–2352018. http://dx.doi.org/10.1103/physrevb.63.235201
20. Li Y., Shi J., Mi Y., Sui X., Xu H., Liu X. Ultrafast carrier dynamics in two-dimensional transition metal dichalcogenides. *J. Mater. Chem. C*, 2019; 7(15): 4304–4319. http://dx.doi.org/10.1039/c8tc06343e
21. Brekhov K.A., Grishunin K.A., Ilyin N.A., Shestakova A.P., Lavrov S.D., Mishina E.D. Optical diagnostics of $WSe_2$ monolayers. *Tech. Phys. Lett.*, 2017; 43(12): 1112–1114. http://dx.doi.org/10.1134/S106378501712015X
22. He K., Kumar N., Zhao L., Wang Z., Mak K.F., Zhao H., Shan J. Tightly bound excitons in monolayer $WSe_2$. *Phys. Rev. Lett.*, 2014; 113(2): 026803. http://dx.doi.org/10.1103/PhysRevLett.113.026803
23. Sabbah A.J., Riffe D.M. Femtosecond pump-probe reflectivity study of silicon carrier dynamics. *Phys. Rev. B*, 2002; 66(16): 1–11. http://dx.doi.org/10.1103/PhysRevB.66.165217
24. Chernikov A., Ruppert C., Hill H.M., Rigosi A.F., Heinz T.F. Population inversion and giant bandgap renormalization in atomically thin $WS_2$ layers. *Nat. Photonics*, 2015; 9(7): 466–470. http://dx.doi.org/10.1038/nphoton.2015.104
25. Dendzik M., Xian R.P., Perfetto E. et al. Observation of an excitonic Mott transition through ultrafast core-*cum*-conduction photoemission spectroscopy. *Phys. Rev. Lett.*, 2020; 125(9): 096401. http://dx.doi.org/10.1103/PhysRevLett.125.096401
26. Burstein E. Anomalous optical absorption limit in InSb. *Phys. Rev.*, 1954; 93(3): 632–633. http://dx.doi.org/10.1103/PhysRev.93.632